Biomol NMR Assign (2014) 8:365–370
DOI 10.1007/s12104-013-9518-y

ARTICLE

Solid-state NMR sequential assignments of the amyloid core of Sup35pNM

Nina Luckgei · Anne K. Schütz · Birgit Habenstein · Luc Bousset · Yannick Sourigues · Ronald Melki · Beat H. Meier · Anja Böckmann

Received: 12 April 2013 / Accepted: 1 August 2013 / Published online: 10 August 2013

Abstract Sup35pNM represents the N-terminal and middle (M) domains of the yeast *Saccharomyces cerevisiae* prion Sup35p. This fragment is commonly used for structural and functional studies of Sup35p. We here present a solid-state NMR study of fibrils formed by this fragment and show that sequential assignments can be obtained for the rigid and well-ordered parts of the protein using 3D spectroscopy. We describe in detail the sequential assignment of the 22 residues yielding strong, narrow signals with chemical shifts that correspond mostly to β-sheet secondary-structured amino acids that form the fibril core.

Keywords Sup35pNM · Fibrils · Solid-state NMR · Assignments · Secondary structure

Nina Luckgei, Anne Schütz, Birgit Habenstein, and Luc Bousset have contributed equally to this work.

N. Luckgei · B. Habenstein · A. Böckmann (✉)
Institut de Biologie et Chimie des Protéines, UMR 5086 CNRS/ Université de Lyon, 1, 7 passage du Vercors,
69367 Lyon, France
e-mail: a.bockmann@ibcp.fr

A. K. Schütz · B. H. Meier (✉)
Physical Chemistry, ETH Zürich, Wolfgang-Pauli-Strasse 10,
8093 Zurich, Switzerland
e-mail: beme@ethz.ch

L. Bousset · Y. Sourigues · R. Melki (✉)
Laboratoire d'Enzymologie et Biochimie Structurales,
UPR 3082 CNRS, Avenue de la Terrasse,
91198 Gif-sur-Yvette, France
e-mail: melki@lebs.cnrs-gif.fr

Biological context

Sup35pNM is an N-terminal fragment of the 685 amino-acid protein Sup35 of *Saccharomyces cerevisiae* that has prion properties at the origin of the [PSI^+] phenotype (Cox 1965; Wickner et al. 1995; Krzewska and Melki 2006; Krzewska et al. 2007). It spans residues 1-253 of Sup35p and comprises the N-terminal domain, essential for prion formation (DePace et al. 1998), as well as the middle domain (M-domain) whose function is yet unknown. While the N-terminal domain (N-domain) is rich in glutamine and asparagine residues, the M-domain consists mainly of charged residues. Sup35pNM forms self-seeding amyloid fibrils in vivo and in vitro under physiological pH and salt concentrations. Sup35pNM is the most extensively studied fragment of the Sup35p prion (Glover et al. 1997; Chien et al. 2005; Krishnan and Lindquist 2005; Toyama et al. 2007; Foo et al. 2011; Verges et al. 2011; Halfmann et al. 2011). Nevertheless, structural studies on the molecular level of Sup35pNM fibrils are scarce since they are not amenable to X-ray crystallography or solution NMR. We present here the solid-state NMR sequential assignments of this protein, as well as a secondary structure analysis, of the well-ordered, rigid parts of the protein. The assignment of the mother protein, namely the full-length prion Sup35p, is described in a companion paper (Schütz et al. 2013). A detailed comparison and a biophysical interpretation of the differences will be presented elsewhere (Luckgei et al. 2013).

Methods and experiments

Protein expression and purification; sample preparation

The protein was expressed and purified as shortly summarized here, and described in detail in (Krzewska and

Melki 2006; Krzewska et al. 2007). The protein has an N-terminal His-tag for purification purposes (for the full amino acid sequence see Fig. 1), and was labeled with ^{13}C and ^{15}N in M9 medium. For fibrillization, Sup35pNM (in 20 mM Tris HCl, pH 8.0, 200 mM NaCl, 5 % glycerol, 5 mM β-mercaptoethanol, 10 mM $MgCl_2$) was incubated at 10 °C under orbital shaking at 30 rpm, 0.5 cm amplitude, for 3 weeks. The fibrils were pelleted at 100,000*g* in a TL-100 tabletop centrifuge for 20 min at 4 °C. The fibrils were resuspended in distilled water, washed twice, and filled into 3.2 mm rotors by ultracentrifugation as described (Böckmann et al. 2009).

NMR spectroscopy

We used a suite of 2D and 3D experiments, namely 2D DARR and DREAM, and 3D NCACB, NCACO, NCACX, NCOCA, NCOCX, CANCO and CCC experiments to perform the assignment as described in detail in references (Schuetz et al. 2010; Habenstein et al. 2011). Each 3D spectrum took between 2 and 5 days to be recorded. The sequential walk was achieved by connecting resonances from NCACO/NCACX, CANCO and NCOCA/NCOCX spectra. Side-chain assignments were performed using NCACB, NCACX, NCOCX and CCC spectra. Full experimental details are given in Table 1. All assignment spectra were recorded on the same sample. However, 2D DARR spectra were recorded for two different preparations to verify reproducibility of the sample preparation.

All spectra were recorded on a Bruker Avance II+850MHz spectrometer operating at a static magnetic field of 20 T. A 3.2 mm Bruker triple-resonance MAS probe equipped with an LLC coil was used to reduce r.f. heating during the experiments. The spectra were recorded at sample temperatures between 5 and 10 °C. The pulse sequences were implemented as recently reported (Schuetz et al. 2010). All spectra were processed using TopSpin 2.0 (Bruker Biospin) by zero filling to the next power of two and the time domain signals were apodized with a squared cosine function. Spectra were analyzed and annotated using the CcpNmr Analysis package (Fogh et al. 2002; Vranken et al. 2005; Stevens et al. 2011).

Assignment and data deposition

Figure 2 shows the 2D NCA and NCO spectra of Sup35pNM. The most intense correlations could be sequentially assigned and are labeled. A sequential assignment was possible for those signals that lead to sufficiently strong signals in the 3D spectra, which indeed reveal only a small subset of the resonances of the residues of the NM domains, due to static and/or dynamic disorder for the remaining parts of the protein. The line widths of the resonances detected in the 3D spectra are mostly between 0.5 and 1 ppm, and the spectra show a good resolution and dispersion (Fig. 3). Assignments were established for all residues with corresponding signals present in the NCACO/CX, CANCO and NCOCA/CX spectra (Schuetz et al. 2010; Habenstein et al. 2011).

To illustrate sequential assignments, a representative plane of the 3D NCACB, NCACO, CANCO and NCOCA experiments is shown in Fig. 3. Shifts for 22 residues could be assigned, which are all located in the N-terminal prion domain. The chemical shifts have been deposited in the BMRB under the accession number 18406.

As a probe for flexibility, highly dynamic residues generally can be detected in INEPT spectra without homonuclear proton decoupling during polarization transfer. For Sup35pNM, all amino-acid types with the exception of Arg, Phe and Tyr could be observed in this scalar-coupling based spectrum, as shown in Fig. 4. The absence of Arg in the spectra coincides with the absence of Arg residues in the M-domain. Also, all residue-types present in the M-domain show signals in the INEPT spectrum.

Assigned resonances are shown in the assignment graph in Fig. 5. As shown in Fig. 2, most strong cross peaks in the 2D NCA spectrum can be explained based on this assignment.

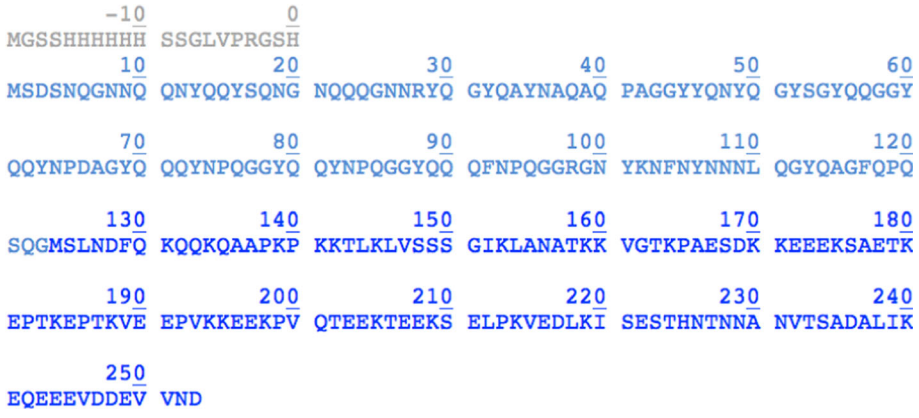

Fig. 1 Amino-acid sequence of the Sup35pNM construct used. The tag is shown in *grey*, the N domain in *light blue*, and the M domain in *deep blue*

Table 1 Experimental parameters

Experiment	DARR 20 ms	DARR 100 ms	NCA	NCO	INEPT
MAS frequency [kHz]	18	17.5	17.5	17.5	18
Transfer 1	HC-CP	HC-CP	HN-CP	HN-CP	INEPT
Field [kHz]-^{1}H	64.7	72.6	55.0	64.7	62.5
Field [kHz]-^{13}C/^{15}N	55.5	63.7	41.6	41.6	50.0
Shape	Tangent ^{1}H	Tangent ^{1}H	Tangent ^{1}H	Tangent ^{1}H	Hard pulses
^{13}C carrier [ppm]	55.6	55.6	–	–	–
Time [ms]	0.5	0.5	0.8	1	
Transfer 2	MIRROR	MIRROR	NC-CP	NC-CP	–
Field [kHz]-^{1}H	5.4	6.1	101.5	101.5	–
Field [kHz]-^{13}C	–	–	10.9	10.9	–
Field [kHz]-^{15}N	–	–	6.6	8.2	–
Shape	–	–	Tangent ^{13}C	Tangent ^{13}C	–
^{13}C carrier [ppm]	–	–	61.2	178.6	–
Time [ms]	20	100	6	6	–
t_1 increments	1,024	1,216	512	256	192
Sweep width (t_1) [kHz]	66.667	80	20	10	10
Max. acq time (t_1) [ms]	7.68	7.60	12.80	12.80	9.60
t_2 increments	2,048	2,048	2,048	2,560	2,048
Sweep width (t_2) [kHz]	100	100	100	100	100
Max. acq time (t_2) [ms]	10.24	10.24	10.24	12.80	10.24
t_3 increments	–	–	–	–	–
Sweep width (t_3) [kHz]	–	–	–	–	–
Max. acq time (t_3) [ms]	–	–	–	–	–
^{1}H Spinal64 Decoupling power [kHz]	100	100	100	100	76.9
Interscan delay [s]	2.5	2.5	2	2	2
Number of scans	8	24	8	8	8
Total measurement time [h]	5.8	21.2	2.3	1.1	0.9

Experiment	NCACB	CANCO	NCOCA	CCC	NCACO	NCACX	NCOCX
MAS frequency [kHz]	17.5	17.5	17.5	17.5	17.5	17.5	17.5
Transfer 1	HN-CP	HC-CP	HN-CP	HC-CP	HN-CP	HN-CP	HN-CP
Field [kHz]-^{1}H	55.0	69.3	67.8	72.6	59.7	67.8	67.8
Field [kHz]-^{13}C/^{15}N	41.6	59.5	43.5	63.7	46.7	44.0	43.5
Shape	Tangent ^{1}H	Tangent ^{1}H	Tangent ^{1}H	Tangent ^{1}H	Tangent ^{1}H	Tangent ^{1}H	Tangent ^{1}H
Carrier [ppm]	–	48.5	–	–	–	–	–
Time [ms]	0.8	0.6	1.2	0.5	0.8	1.2	1.2
Transfer 2	NC-CP	CN-CP	NC-CP	DREAM	NC-CP	NC-CP	NC-CP
Field [kHz]-^{1}H	101.5	116.6	82.5	101.5	101.5	102.7	82.5
Field [kHz]-^{13}C	10.9	11.0	11.0	8.3	10.5	11.0	11.0
Field [kHz]-^{15}N	6.6	6.8	8.1	–	8.3	7.2	8.1
Shape	Tangent ^{13}C	Tangent ^{13}C	Tangent ^{13}C	Tangent ^{13}C	tangent ^{13}C	tangent ^{13}C	tangent ^{13}C
Carrier [ppm]	61.2	61.6	178.6	55.0	57.9	57.9	178.6
Time [ms]	6	8	5	4	5.5	6.5	5
Transfer 3	DREAM	NC-CP	MIRROR	MIRROR	MIRROR	MIRROR	MIRROR
Field [kHz]-^{1}H	–	–	21.8	3.4	21.3	3.2	21.8
Field [kHz]-^{13}C	8.0	11.0	–	–	–	–	–
Field [kHz]-^{15}N	–	8.2	–	–	–	–	–
Shape	tangent^{13}C	tangent^{13}C	–		–	–	–
Carrier [ppm]	59.0	178.6	–	–	–	–	–

Table 1 continued

Experiment	NCACB	CANCO	NCOCA	CCC	NCACO	NCACX	NCOCX
Time [ms]	4	6	80	200	20	80	80
T_1 increments	128	128	80	216	80	80	80
Sweep width (t_1) [kHz]	6.8	10	4	20	4	4	4
Max. acq time (t_1) [ms]	9.4	6.4	10	5.4	10	10	10.00
t_2 increments	96	96	96	216	96	128	96
Sweep width (t_2) [kHz]	9.6	4.8	8	20	8	10	8
Max. acq time (t_2) [ms]	5	10	6	5.4	6	6.4	6.00
t_3 increments	1,536	2,048	2,048	2,048	2,048	2,048	2,048
Sweep width (t_3) [kHz]	100	100	100	100	100	100	100
Max. acq time (t_3) [ms]	7.3	10.3	10.3	10.3	10.3	10.3	10.0
^{1}H Spinal64 Decoupling power [kHz]	100	100	100	100	100	100	100
Interscan delay [s]	2.22	2.45	2.3	1.9	2.3	1.94	2.3
Number of scans	8	8	16	4	16	8	16
Total measurement time [h]	61.2	67.7	81.9	109.6	79.9	46.4	81.7

All spectra were recorded with 850 MHz WB Bruker spectrometer between 5 and 10 °C

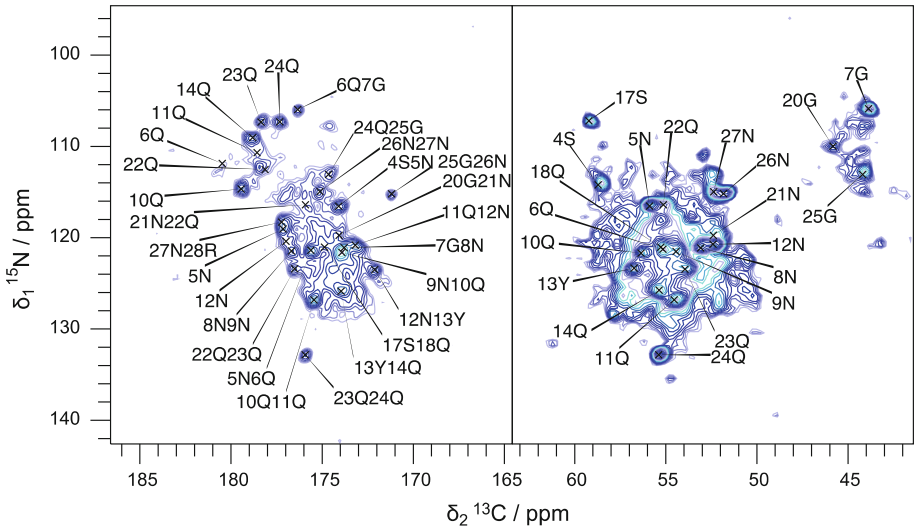

Fig. 2 2D NCA and NCO spectra of Sup35pNM with the sequentially assigned residues labeled. The spectra were acquired at 850 MHz with MAS at 17.5 kHz

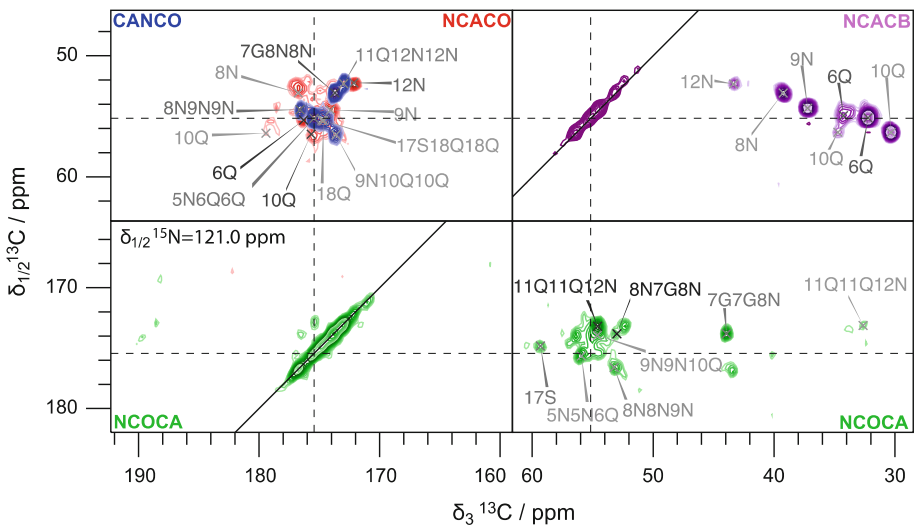

Fig. 3 Representative planes of 3D NCACB, NCACO, CANCO and NCOCA spectra of Sup35pNM with the sequentially assigned residues labeled. Residues labeled in *grey* have the center of the peak in another plane. Dotted lines highlight the connection between Q6 and N5

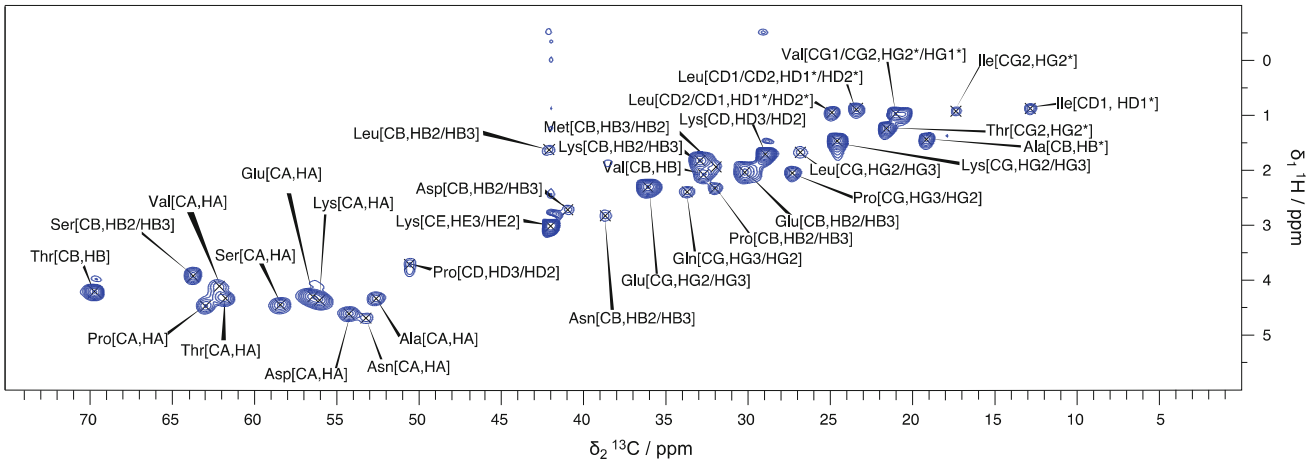

Fig. 4 INEPT spectrum of Sup35pNM. Signals are assigned to residue types according to the random coil chemical shifts (Wang and Jardetzky 2002)

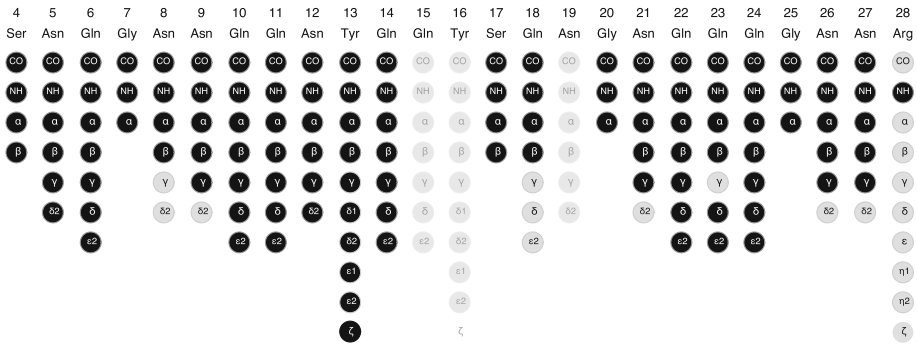

Fig. 5 Assignment graph (created using the CcpNmr software (Fogh et al. 2002; Vranken et al. 2005; Stevens et al. 2011)) of the N-terminal amino acids of Sup35pNM

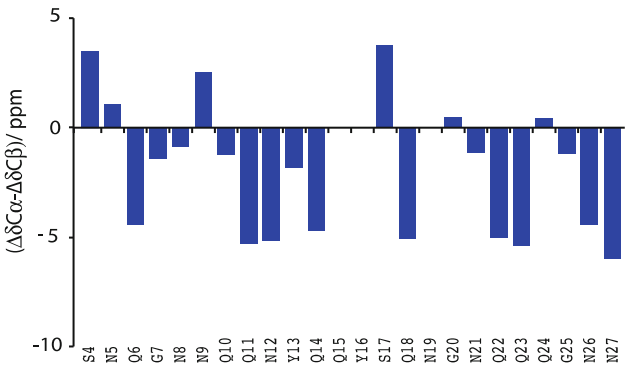

Fig. 6 Secondary chemical shifts for Sup35pNM. Secondary chemical shifts have been calculated as given in (Wishart and Sykes 1994) and we report the difference between Cα and Cβ secondary shifts (Luca et al. 2001). Three or more negative values in a row suggest β-strand conformation. Isolated positive or negative values for a given residue suggest turn or random-coil conformation. For Gly, the secondary shift of Cα is plotted

The secondary chemical shifts for the assigned residues are given in Fig. 6. The assigned residues mostly display secondary chemical shifts typical for β-strand conformation. For glycines, only ΔδCα is plotted.

The sequential assignments of the rigid and well-ordered amino acids of Sup35pNM represent a first step towards the structural analysis of this prion.

Acknowledgments We thank Dr. Christian Wasmer for help with recording the spectra. This work was supported by the Agence Nationale de la Recherche (ANR-12-BS08-0013-01), the ETH Zurich, the Swiss National Science Foundation (Grant 200020_124611) and the Centre National de la Recherche Scientifique. We also acknowledge support from the European Commission under the Seventh Framework Programme (FP7), contract Bio-NMR 261863.

References

Böckmann A, Gardiennet C, Verel R, Hunkeler A, Loquet A, Pintacuda G, Emsley L, Meier BH, Lesage A (2009) Characterization of different water pools in solid-state NMR protein samples. J Biomol NMR 45(3):319–327

Chien P, Yonekura K, Weissman J (2005) Mechanism of cross-species prion transmission: an infectious conformation compatible with two highly divergent yeast prion proteins. Cell 121:49–62

Cox BS (1965) Psi, a cytoplasmic suppressor of super-suppressor in yeast. Heredity 20(4):505–521

DePace AH, Santoso A, Hillner P, Weissman JS (1998) A critical role for amino-terminal glutamine/asparagine repeats in the formation and propagation of a yeast prion. Cell 93(7):1241–1252

Fogh R, Ionides J, Ulrich E, Boucher W, Vranken W, Linge JP, Habeck M, Rieping W, Bhat TN, Westbrook J, Henrick K, Gilliland G, Berman H, Thornton J, Nilges M, Markley J, Laue E (2002) The CCPN project: an interim report on a data model for the NMR community. Nat Struct Biol 9(6):416–418

Foo CK, Ohhashi Y, Kelly MJS, Tanaka M, Weissman JS (2011) Radically different amyloid conformations dictate the seeding specificity of a chimeric Sup35 prion. J Mol Biol 408(1):1–8

Glover JR, Kowal AS, Schirmer EC, Patino MM, Liu JJ, Lindquist S (1997) Self-seeded fibers formed by Sup35, the protein determinant of [PSI+], a heritable prion-like factor of *S. cerevisiae*. Cell 89(5):811–819

Habenstein B, Wasmer C, Bousset L, Sourigues Y, Schütz A, Loquet A, Meier BH, Melki R, Böckmann A (2011) Extensive de novo solid-state NMR assignments of the 33 kDa C-terminal domain of the Ure2 prion. J Biomol NMR 51(3):235–243

Halfmann R, Alberti S, Krishnan R, Lyle N, O'Donnell CW, Donnell CW, King OD, Berger B, Pappu RV, Lindquist S (2011) Opposing effects of glutamine and asparagine govern prion formation by intrinsically disordered proteins. Mol Cell 43(1):72–84

Krishnan R, Lindquist S (2005) Structural insights into a yeast prion illuminate nucleation and strain diversity. Nature 435(7043): 765–772

Krzewska J, Melki R (2006) Molecular chaperones and the assembly of the prion Sup35p, an in vitro study. EMBO J 25(4):822–833

Krzewska J, Tanaka M, Burston SG, Melki R (2007) Biochemical and functional analysis of the assembly of full-length Sup35p and its prion-forming domain. J Biol Chem 282(3):1679–1686

Luca S, Filippov D, van Boom J, Oschkinat H, de Groot H, Baldus M (2001) Secondary chemical shifts in immobilized peptides and proteins: a qualitative basis for structure refinement under magic angle spinning. J Biomol NMR 20(4):325–331

Luckgei N, Schütz AK, Bousset L, Habenstein B, Sourigues Y, Gardiennet C, Meier BH, Melki R, Böckmann A (2013) The conformation of the prion domain of Sup35p in isolation and in the full-length protein is different (under review)

Schuetz A, Wasmer C, Habenstein B, Verel R, Greenwald J, Riek R, Böckmann A, Meier BH (2010) Protocols for the sequential solid-state NMR spectroscopic assignment of a uniformly labeled 25 kDa protein: HET-s (1-227). ChemBioChem 11(11):1543–1551

Schütz AK, Habenstein B, Luckgei N, Bousset L, Sourigues Y, Nielsen AB, Melki R, Böckmann A, Meier BH (2013) Solid-state NMR sequential assignments of the amyloid core of full-length Sup35p (submitted)

Stevens TJ, Fogh RH, Boucher W, Higman VA, Eisenmenger F, Bardiaux B, van Rossum B-J, Oschkinat H, Laue ED (2011) A software framework for analysing solid-state MAS NMR data. J Biomol NMR 51(4):437–447

Toyama B, Kelly M, Gross J, Weissman J (2007) The structural basis of yeast prion strain variants. Nature 449(7159):233–237

Verges KJ, Smith MH, Toyama BH, Weissman JS (2011) Strain conformation, primary structure and the propagation of the yeast prion [PSI+]. Nat Struct Mol Biol 18(4):493–499

Vranken W, Boucher W, Stevens T, Fogh R, Pajon A, Llinas P, Ulrich E, Markley J, Ionides J, Laue E (2005) The CCPN data model for NMR spectroscopy: development of a software pipeline. Proteins 59(4):687–696

Wang Y, Jardetzky O (2002) Probability-based protein secondary structure identification using combined NMR chemical-shift data. Protein Sci 11(4):852–861

Wickner RB, Masison DC, Edskes HK (1995) [PSI] and [URE3] as yeast prions. Yeast 11(16):1671–1685

Wishart DS, Sykes BD (1994) The 13C chemical-shift index: a simple method for the identification of protein secondary structure using 13C chemical-shift data. J Biomol NMR 4(2):171–180